Suppression or enhancement of quantum tunneling by a nonlinear resonance induced in a driven double-well system

Ju-Yong Shin
Department of Physics, Korea Advanced Institute of Science and Technology, Taejon, 305-701, South Korea
(Received 29 January 1996)

The effect of a periodic driving force on coherent tunneling of a driven double square-well system, especially when its central potential barrier is very tall and very thin, is investigated. The suppression or enhancement of the tunneling of a wave packet properly chosen in the double-well system may be achieved by a judicious choice of the period of a driving force, i.e., by a particular choice of the generating condition of a nonlinear resonance exhibiting a desirable property. We analyze this mechanism by exploiting both the properties of a dynamical symmetry of the Hamiltonian and the localized properties of Floquet states induced by the nonlinear resonance. [S1063-651X(96)06807-9]

PACS number(s): 05.45.+b, 73.40.Gk, 47.52.+j, 03.65.−w

I. INTRODUCTION

The study of quantum dynamical tunneling for double-well systems in the presence of a periodic driving force is a subject currently under intense investigation. The application of a periodic driving force to the tunneling systems generates a variety of complex behaviors. As a result, the interplay between chaos and tunneling is the subject of recent work by many researchers [1–7]. A wave packet initially centered on one of the symmetric Kolmogorov-Arnold-Moser (KAM) islands can tunnel through the chaotic sea to reach the other KAM island, and then return to the original island. This kind of quantum dynamical tunneling between the disconnected symmetric KAM islands first studied by Davis and Heller [8], has been under recent study.

Now, it was discovered by Lin and Ballentine [9] that for certain values of the driving force parameters, the tunneling rate can be enhanced by many orders of magnitude compared with the undriven rate. Peres [10] pointed out that the observed tunneling is due to a dynamical symmetry of the Hamiltonian, which remains invariant under combined spatial reflection and time translation. However, the dynamical symmetry cannot sufficiently explain why the Floquet states should, in some cases but not in others, be approximately localized in the regular regions of classical phase space [11]. It might be explained by studying the characteristics of nonlinear resonances induced by a periodic driving force. In this case, Lin and Ballentine [12] found that the tunneling times of the localized Floquet state between the resonant islands become rather erratic with the increase of the amplitude of the driving force. Perhaps this can be ascribed to a mechanism of chaos-induced avoided level crossing between the Floquet states associated with the chaotic part of phase space and a member of the quasidegenerate doublet [13]. On the other hand, it was independently shown in the deep quantum regime by Grossmann *et al.* [14–17] that the driving parameters can also be adjusted to reduce the tunneling rate to zero. The total inhibition of the tunneling occurs at the exact crossing of the two levels for the even and the odd Floquet states.

To control tunneling properties of systems, these properties of enhancement and suppression of tunneling have been applied. Bavli and Metiu [18] showed that a semi-infinite laser pulse can be used to localize an electron in one of the wells of a double-well potential with the suppression mechanism of tunneling in the deep quantum regime. An alternative way of suppressing tunneling is to destroy the discrete symmetry itself. Farrelly and Milligan [19] also revealed this by combining the mechanism with the result studied by Lin and Ballentine, that is to say, the control and suppression of tunneling is achieved by driving the system with two fields whose frequencies are a 1:2 ratio.

In this paper, we will show an example of a control system of tunneling which uses a different mechanism from the ones described above and then study its properties in a not so deep quantum regime and weakly chaotic regime. We will discuss how to select an initial wave packet whose coherent tunneling is capable of being controlled by an appropriate choice of a period of the driving force in a driven double square-well system when its central barrier is very tall and very thin. Patterns of regular islands in the Poincaré surface of section rest on the period of the driving force, the amplitude of the driving force, and other variables. In this case, the property of a regular island, especially the property of a stable fixed point of a regular island, is well described by the property of the corresponding nonlinear resonance. Accordingly, if we control the generating condition of a nonlinear resonance exhibiting the property that suppresses or enhances the tunneling of the system, we can control the tunneling of the system.

Section II begins with a description of our model system. Section III examines the properties of a tunnel controlling system by changing the period of the driving force in a double square-well system. Section IV analyzes the mechanism of suppressed tunneling and enhanced tunneling by studying the properties of dynamical symmetry of the Hamiltonian and localized Floquet states induced by a nonlinear resonance. Section V draws some concluding remarks.

II. SYSTEM

We study dynamical properties of a localized wave packet affected by a coherent driving force $F\cos(2\pi t/T)$ in a double square-well potential $V(q)$,

$$V(q)=\begin{cases}\infty, & \text{for } |q|\geqslant a,\\ 0, & \text{for } b<|q|<a,\\ V_0, & \text{for } |q|\leqslant b.\end{cases} \tag{1}$$

To observe the motion of the wave packet and obtain the time-evolution unitary matrix of the wave packet, we integrate numerically the time-dependent Schrödinger equation,

$$i\hbar\frac{dc_n(t)}{dt}=\sum_{m=1} F\cos\left(\frac{2\pi t}{T}\right)\langle u_n|q|u_m\rangle c_m(t)e^{i(E_n-E_m)t/\hbar}, \tag{2}$$

which is derived from the Hamiltonian H of the system,

$$H=-\frac{\hbar^2}{2\mu}\frac{\partial^2}{\partial q^2}+V(q)+qF\cos\left(\frac{2\pi t}{T}\right)\equiv H_0+qF\cos\left(\frac{2\pi t}{T}\right), \tag{3}$$

and the total wave function $\psi(q,t)=\Sigma_{n=1}c_n(t)u_n(q)e^{-iE_nt/\hbar}$, where the E_n and the $u_n(q)$ are the nth eigenvalue and the nth eigenfunction of H_0, respectively. In the absence of the driving force, we get numerically the eigenvalue E_n and the eigenfunction u_n presented by a sine or hyperbolic sine function. The parameters used in this paper are the mass $\mu=1$, the Planck constant $\hbar=1$, the potential width $2a=8$, the height of the central potential barrier $V_0=500$, the width of the central potential barrier $2b$, the amplitude of driving force F, and the period of the driving force T.

In this case, $V_0\approx E_{81}$, and the mean energy of eigenstates or Floquet states, which we will discuss in this paper, is approximately $\sim E_{40}$. On the one hand, the diffusive tunneling from one well to the other by global chaos is possible when $F>100$, but we only treat our system when $F\leqslant 6$. Period-1 resonance in the single square-well system discussed in Sec. IV B undergoes global chaos by resonance overlap when the amplitude of the driving force is greater than the critical value $F_c\simeq 6.3$, while the critical value of period-1/2 resonance in the double square-well system discussed in Sec. IV A is approximately $F_c\simeq 12.5$. Because the shape of the potential in our system is stiffer than that of the harmonic potential, chaotic properties are observed more easily in a lower energy region when the amplitude of the driving force is small.

To compare the properties of a quantum resonance with those of a classical resonance manifested in the Poincaré surface of section, we compute the Husimi function $P_H(q_0,p_0,t)$ of a wave packet $\psi(q,t)$ defined as [20–22]

$$P_H(q_0,p_0,t)=\frac{1}{2\pi\hbar}|\langle\varphi_{q_0,p_0}(q)|\psi(q,t)\rangle|^2 \tag{4}$$

$$\varphi_{q_0,p_0}(q)=\left[\frac{\kappa}{\hbar\pi}\right]^{1/4}\exp\left[i\frac{p_0q}{\hbar}-\frac{\kappa(q-q_0)^2}{2\hbar}\right], \tag{5}$$

where κ is the coarse graining parameter. For all the Husimi functions displayed in this paper, $\kappa=1.5$.

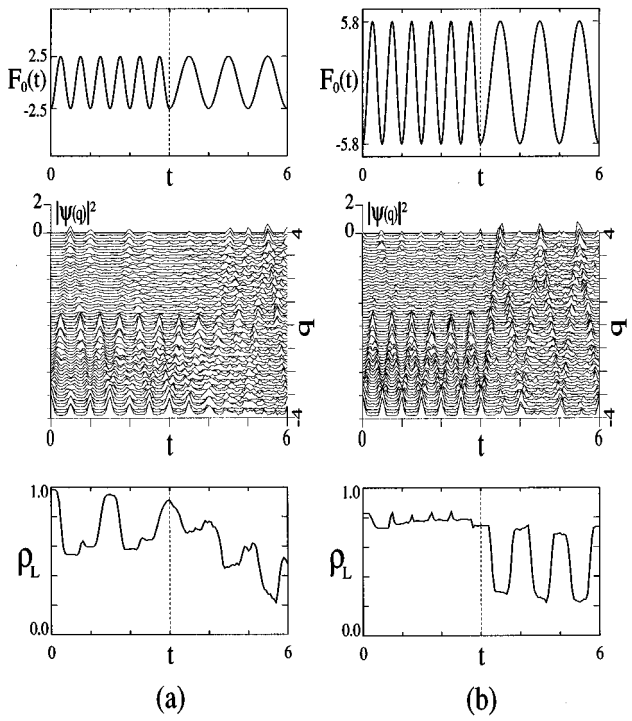

FIG. 1. An example of a tunnel controlling system. The driving force $F_0(t)=-F\cos(2\pi t/T)$, the absolute square of the value of the wave packet $|\psi(q,t)|^2$ and the occupation probability of $|\psi(q,t)|^2$ in the left well $\rho_L(t)$ are drawn, respectively, in the top, middle, and bottom. The results of suppressed tunneling and enhanced tunneling are shown at the time intervals (0,3) and (3,6), respectively. The result is more evident in (b) than in (a). (a) ($T=1/2$ or 1, $F=2.5$, $2b=0.03$, $\mu=1$, $\hbar=1$, $2a=8$, $V_0=500$), (b) ($T=1/2$ or 1, $F=5.8$, $2b=0.03$, $\mu=1$, $\hbar=1$, $2a=8$, $V_0=500$) (in arbitrary units).

III. AN EXAMPLE OF THE TUNNEL CONTROLLING SYSTEM

Figure 1 shows a possibility that the tunneling of an initially localized wave packet $\psi(q,t)$ is capable of being controlled by the change of the period of a sinusoidal driving force in a tunnel controlling system. Or rather, the wave packet undergoes suppressed tunneling at the time interval (0,3), and enhanced tunneling at the time interval (3,6), as the period of the driving force $F_0(t)=-F\cos(2\pi t/T)$ is changed from $T=1/2$ to $T=1$. The driving force $F_0(t)$, the absolute square of the value of the wave packet $|\psi(q,t)|^2$, and the occupation probability of $|\psi(q,t)|^2$ in the left well $\rho_L(t)$ are drawn in the top, middle and bottom of Fig. 1, respectively. The occupation probability $\rho_L(t)$ [14] is defined as

$$\rho_L(t)=\int_{q=-a=-4}^{q=-b\approx 0} dq|\psi(q,t)|^2. \tag{6}$$

When the wave packet $\psi(q,t)$ is affected by the driving force, the values of $|\psi(q,t)|^2$ and $\rho_L(t)$ present the results of a controlled tunneling well. When the controlling system is perturbed by a driving force of a different amplitude, i.e., as in (a) where $F_0(t)=-2.5\cos(2\pi t/T)$, or in (b) where $F_0(t)=-5.8\cos(2\pi t/T)$, the efficiency of the tunnel control-

ling is better in the latter case. Thus, we first describe the properties of the $|\psi(q,t)|^2$ and the $\rho_L(t)$ of Fig. 1(b), and then briefly describe those of Fig. 1(a).

In Fig. 1(b), at the time interval (0,3), the main peak of $|\psi(q,t)|^2$ oscillates with a period 1/2 between the left side potential wall on $(q=-4)$ and the central potential barrier on $(q\approx 0)$. Whereas, at the time interval (3,6), the main peak oscillates with a period 1 between the two potential walls on $(q=\pm 4)$ of double wells. These results imply that at the time interval (0,3) most of the probability of $|\psi(q,t)|^2$ is confined in the left well because the tunneling effect of $|\psi(q,t)|^2$ through the central potential barrier is extremely minute, while at the time interval (3,6) most of the probability of $|\psi(q,t)|^2$ oscillates between both wells through the central potential barrier because the tunneling effect of $|\psi(q,t)|^2$ through the central potential barrier is rather dominant. The occupation probability $\rho_L(t)$ in the bottom of Fig. 1 helps us make a decision whether most of the probability of $|\psi(q,t)|^2$ remains within the left side well (or right side well) or oscillates between the two wells through the central barrier. In Fig. 1(b), at the time interval (0,3) the value of $\rho_L(t)$ larger than 0.73 manifests the results of suppressed tunneling of $\psi(q,t)$ through the central barrier. Whereas, at the time interval (3,6), the strong oscillation of the value of $\rho_L(t)$ manifests the results of enhanced tunneling of $\psi(q,t)$ through the central barrier.

The results of suppressed tunneling and enhanced tunneling presented in Fig. 1(a) are less evident than those presented in Fig. 1(b). For example, at the time interval (0,3), the minimum value 0.54 of $\rho_L(t)$ in Fig. 1(a) is smaller than the minimum value 0.73 in Fig. 1(b); in addition, at the time interval (3,6) the oscillatory motion of the value of $\rho_L(t)$ is less evident in Fig. 1(a). These imply that the mechanism of suppressed tunneling and enhanced tunneling may be more dominant when the amplitude of the driving force is large.

In summary, if the system is driven by $F_0(t)=-F\cos[2\pi t/(1/2)]$, most of the wave packet initially localized in the left well oscillates within the left well of the double wells with the same period as the driving force. Whereas, if the system is driven by $F_0(t)=-F\cos[2\pi t/(1)]$, most of the wave packet oscillates through the central barrier within the double wells with the same period as the driving force.

IV. FLOQUET ANALYSIS OF NONLINEAR RESONANCES

In this section, we analyze the mechanism of suppressed tunneling and enhanced tunneling, i.e., the results of Sec. III with the supporting aid of the Floquet analysis [23–25] of the properties of nonlinear resonances [26–28] induced by the driving force and the property of the dynamical symmetry [10,29,30] of the Hamiltonian.

A. Tunnel suppression induced by a period-1/2 resonance

Most of the mechanism of suppressed tunneling at the time interval (0,3) presented in Fig. 1 can be explained by the property of the dynamical quasidegeneracies [31,32] of the nearly degenerated doublet states associated with the stable fixed point of the period-1/2 resonance generated by the driving force, $F_0=-F\cos[2\pi t/(1/2)]$. Thus we will first examine the interplay between the properties of the nearly degenerated doublet state and period-1/2 nonlinear resonance induced by the driving force of $F_0=-2.5\cos(4\pi t)$.

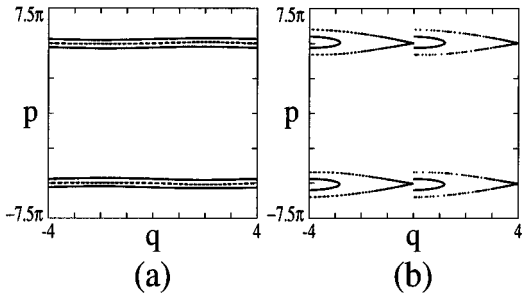

FIG. 2. Classical Poincaré surface of section in a driven single or double square-well system is drawn in (a) or (b), respectively. The regular islands are clear in (b) but not in (a). (a) $(T=1/2,\ F=2.5,\ 2b=0.00,\ \mu=1,\ \hbar=1,\ 2a=8,\ V_0=0)$, (b) $(T=1/2,\ F=2.5,\ 2b=0.03,\ \mu=1,\ \hbar=1,\ 2a=8,\ V_0=500)$.

When the classical system is driven by a sinusoidal force, profoundly different aspects are manifested in the specifically considered portion of the Poincaré surface of section depending on whether it has the central potential barrier or not, even though the thickness of the barrier is extremely thin. With the central potential barrier, the islands of the period-1/2 resonance are clearly manifested in the Poincaré surface of section as in Fig. 2(b), while, without the barrier, the islands are not manifested as in Fig. 2(a). If we observe Husimi functions of some Floquet states, we also find the trace of the period-1/2 resonance in the quantum system. Husimi functions of Floquet states in Fig. 3(b) illustrate the trace of the period-1/2 resonance. However, the trace is not discovered in Fig. 3(a) as in Fig. 2(a). The χ_i's in Fig. 3 are some of the Floquet states obtained by diagonalizing the time-evolution unitary matrix of a wave function [33], which are sorted with respect to the expectation value of their mean momentum, defined as $\langle p_i\rangle=\sqrt{2\mu\langle\chi_i|H_0|\chi_i\rangle}$. The χ_i's in Figs. 3(a) and 3(b) are calculated for the same value of the system parameters as in Figs. 2(a) and 2(b). The χ_{40} and χ_{41} of Fig. 3(b) are, respectively, even and odd states of one nearly degenerated doublet with respect to a parity operator [10], which best displays the property of two stable fixed points of the period-1/2 resonance of Fig. 2(b).

If the initial wave packet is composed of more than one nearly degenerated doublet state, time evolution of the wave packet may be very complicated and Fourier analysis needs to be applied [12]. However, if the initial wave packet is composed of only one nearly degenerated doublet state, the tunneling time of the wave packet is then easily determined.

One purpose of this paper is to make the property of time evolution of an initial wave packet follow the dynamical property of the one nearly degenerated doublet, i.e., the pair of χ_{40} and χ_{41}, when the wave packet undergoes suppressed tunneling by the driving force as in Fig. 1 because we can suppress tunneling of the wave packet by controlling the tunneling time of the doublet. Moreover, the property of the doublet associated with the stable fixed points stands for the global property of the two islands of period-1/2 resonance. Therefore we first examine the time evolution of the wave packet initially composed of the one nearly degenerated dou-

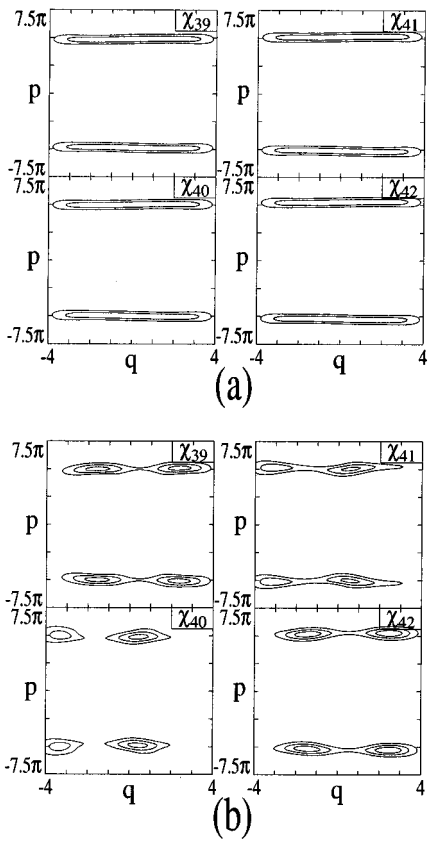

FIG. 3. The Husimi functions of some Floquet states compared with the classical Poincaré surface of sections in Fig. 2. The trace of regular islands of nonlinear resonance is shown in the Husimi functions drawn in (b) but not in (a). The χ_{40} and χ_{41} of (b) are, respectively, even and odd states of one nearly degenerated doublet with respect to a parity operator, which displays the property of two stable fixed points of the period-1/2 resonance of Fig. 2(b). The Husimi functions are calculated for the same values of the system parameters as in Figs. 2(a) and 2(b).

blet. Most of the motion of the wave packet undergoing suppressed tunneling in Fig. 1 can be described by the dynamical property of the linear combination of the one nearly degenerated doublet, i.e., the pair of χ_{40} and χ_{41}. If we choose a symmetric combination of these two Floquet states as

$$\psi_S(q,0)=\frac{1}{\sqrt{2}}[\chi_{40}(q,t=0)+\chi_{41}(q,t=0)] \equiv \frac{1}{\sqrt{2}}[\chi_{40}(q)+\chi_{41}(q)], \tag{7}$$

the time evolution of the $\psi_S(q,nT)$ at times corresponding to integral multiples of a period $T=1/2$ of the driving force is given by [10,26]

$$\psi_S(q,nT)=\frac{1}{\sqrt{2}}[\chi_{40}(q)+\chi_{41}(q)e^{-i(\epsilon_{41}-\epsilon_{40})nT/\hbar}]e^{-i\epsilon_{40}nT/\hbar} \tag{8}$$

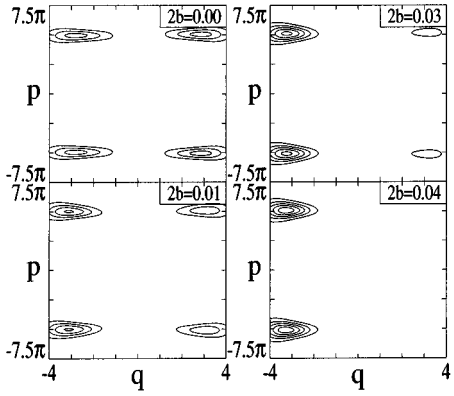

FIG. 4. Observation of the localization of the Husimi function of a wave packet $\psi_S(q,0)$ composed of the linear combination of one nearly degenerated doublet associated with χ_{40} and χ_{41} in Fig. 3(b). When the amplitude of thickness of the central potential barrier is increased as $2b=0.00$, 0.01, 0.03, and 0.04, the Husimi function is more strongly localized about the stable fixed point of the resonance in the left well. ($T=1/2$, $F=2.5$, $\mu=1$, $\hbar=1$, $2a=8$, $V_0=500$).

and the time evolution of the $\psi_S(q,nT+T/2)$ at times corresponding to integral multiples of the period plus one-half period is given by [26]

$$\psi_S(q,nT+T/2)=\frac{1}{\sqrt{2}}[\chi_{40}(-q) -\chi_{41}(-q)e^{-i(\epsilon_{41}-\epsilon_{40})(nT+T/2)/\hbar}] \times e^{-i\epsilon_{40}(nT+T/2)/\hbar}. \tag{9}$$

This equation is ascribed to the property $\chi_n(q,nT+T/2)=\pm\chi_n(-q,t=0)$ which is derived from the dynamical symmetry of the Hamiltonian. Namely, it is satisfied that $\chi_{40}(q,t=T/2)=\chi_{40}(-q,t=0)$ for the even parity state χ_{40}, and $\chi_{41}(q,t=T/2)=-\chi_{41}(-q,t=0)$ for the odd parity state χ_{41} [12]. Since Eqs. (8) and (9) outline most of the mechanism related to the suppressed tunneling, let us briefly examine the meaning represented by those equations. The tunneling time of $\psi_S(q,t)$, $\tau=\pi/|\epsilon_{41}-\epsilon_{40}|\equiv\pi/\Delta\epsilon$, is derived from the condition $|\epsilon_{41}-\epsilon_{40}|\tau/\hbar=\pi$ in the phase factor of Eq. (8). Therefore, the time evolution of the wave packet $\psi_S(q,t)$ exhibits the oscillatory motion of coherent tunneling between two symmetric KAM islands with a period 2τ.

Before going into detailed descriptions of the motion of coherent tunneling, let us first examine the localization pattern of the Husimi function of the linear combination of one doublet, i.e., $\psi_S(q,t=0)$. As shown in Fig. 4, Husimi functions of $\psi_S(q,t=0)$ are better localized in the left well with the increase in thickness of the central potential barrier as $2b=0.00,0.01,0.03,0.04$. In this case, the pattern of one KAM island of period-1/2 resonance generated in the left well is displayed best when $2b=0.04$. This is ascribed to the fact that the generating condition of the period-1/2 resonance requires the role of the central potential barrier as shown in Figs. 2 and 3.

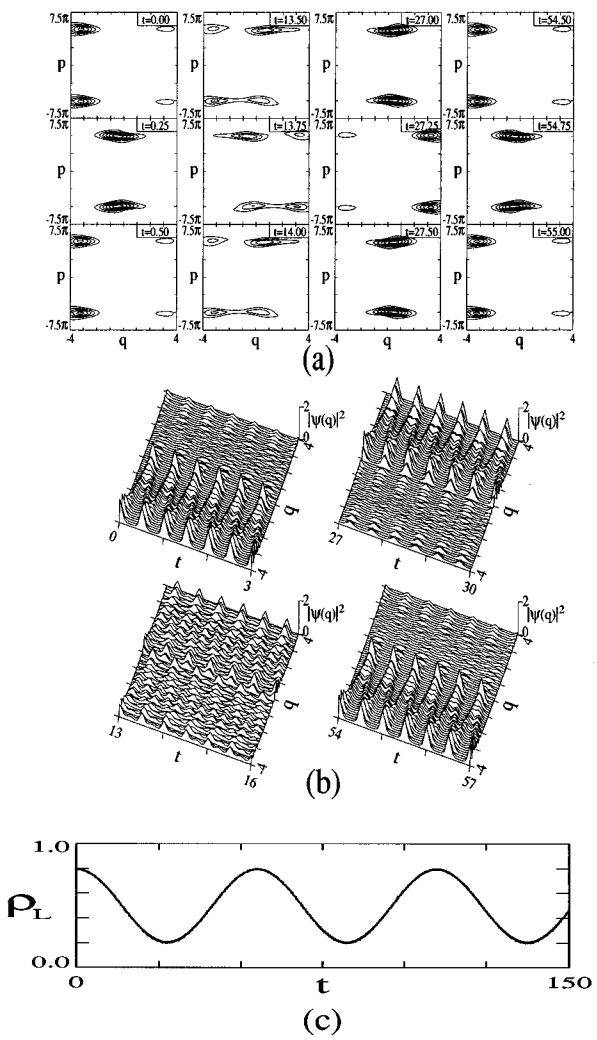

FIG. 5. Time evolution of a wave packet of $\psi_S(q,t)$ chosen in Fig. 4 when $2b=0.03$. Husimi functions of $\psi_S(q,t)$ at selected times corresponding to integral multiples of half period of the driving force are drawn in (a), the time evolution of $|\psi_S(q,t)|^2$ for short time intervals are drawn in (b), and the occupation probability in the left well $\rho_L(t)$ is drawn in (c). The detailed descriptions are given in the contents. ($T=1/2$, $F=2.5$, $2b=0.03$, $\mu=1$, $\hbar=1$, $2a=8$, $V_0=500$).

Taking a wave packet of $\psi_S(q,t=0)$ in case $2b=0.03$ drawn in Fig. 4 as an initial wave packet, we describe in many ways the time evolution of the $\psi_S(q,t)$ in Fig. 5. The tunneling time is given by $\tau=\pi/\Delta\epsilon\approx\pi/0.114\approx27.5=55T$ from Fig. 7, in the case of the parameters of $F=2.5$, $T=1/2$, $2b=0.03$. The oscillatory motion of coherent tunneling with a period ($2\tau\approx55$) is well manifested in the plot of the occupation probability in the left well $\rho_L(t)$ drawn in Fig. 5(c). The minimum value of $\rho_L(t)$ at time ($t=\tau\approx27.5$) means that, as the result of coherent tunneling, most of the probability of $\psi_S(q,t)$ is observed in the right well of ($0\leqslant q\leqslant4$), while the maximum value of $\rho_L(t)$ at time ($t=2\tau\approx55$) means most of the probability of $\psi_S(q,t)$ is again observed in the left well of ($-4\leqslant q\leqslant0$). At time ($t=\tau/2\approx13.7$) corresponding to $\rho_L(t)=0.5$, each well has half the probability of $\psi_S(q,t)$.

For a more detailed description of the time evolution of

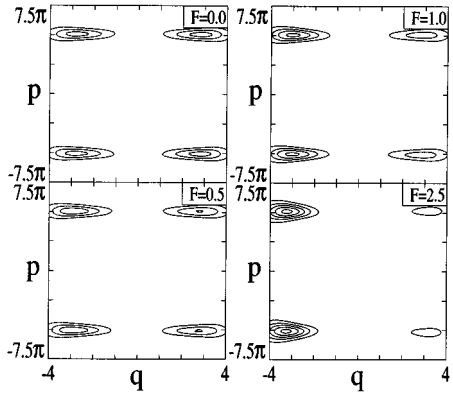

FIG. 6. Observation of the localization of the Husimi function of a wave packet of $\psi_S(q,0)$ composed of the linear combination of one nearly degenerated doublet associated with χ_{40} and χ_{41} in Fig. 3(b). When the amplitude of the driving force is increased as $F=0.0$, 0.5, 1.0, and 2.5, the Husimi function is more strongly localized around the stable fixed point of the period-1/2 resonance in the left well. ($T=1/2$, $2b=0.03$, $\mu=1$, $\hbar=1$, $2a=8$, $V_0=500$).

$\psi_S(q,t)$ when $t=0$, $\tau/2$, τ, and 2τ, we present the time evolution of $|\psi_S(q,t)|^2$ for short time intervals in Fig. 5(b). The motion of the wave packet of $|\psi_S(q,t)|^2$ can be described by the fast oscillation with the same period 1/2 as the driving force. The fast oscillation of the period $T=1/2$ corresponds to the classical oscillation of a particle within each one of the double wells.

To elucidate the property of the time evolution of $\psi_S(q,t)$, in Fig. 5(a), we observe the Husimi functions of $\psi_S(q,t)$ when they correspond to integral multiples of the half period of the driving force. The motion of the Husimi function at those times is described by Eqs. (8) and (9). The $\psi_S(q,nT+T)$ is not much different from $\psi_S(q,nT)e^{-i\epsilon_{40}T/\hbar}$ in Fig. 5(a), which can be confirmed by Eq. (8), since $T=0.5\ll\tau/2\approx13.8$. In fact, the Husimi function of $\psi_S(q,nT)$ is similar to $\psi_S(q,0)e^{-i\epsilon_{40}nT/\hbar}$ if the condition ($nT\ll\tau/2$) is satisfied. Accordingly, in Fig. 5(a) the Husimi functions at times ($t=0$) and ($t=T=0.50$) are nearly identical. In this system, the total phase factor of

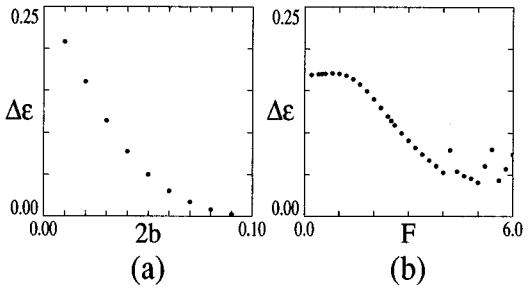

FIG. 7. The change of the tunnel splitting $\Delta\epsilon$ of $\psi_S(q,0)$. The tunnel splitting is reduced with the increase of the amplitude of the thickness of the central barrier as in (a) or with the increase of the amplitude of the driving force F as in (b). (a) ($T=1/2$, $F=2.5$, $\mu=1$, $\hbar=1$, $2a=8$, $V_0=500$), (b) ($T=1/2$, $2b=0.03$, $\mu=1$, $\hbar=1$, $2a=8$, $V_0=500$).

$\psi_S(q,t)$ has no significance. Therefore, for a short time, we can treat the wave packet of $\psi_S(q,nT)$ as an eigenstate. Or rather, we can treat the $\psi_S(q,nT)$ as an eigenstate undergoing suppressed tunneling, as in Fig. 1, if we consider the time evolution of the $\psi_S(q,nT)$ only within a time interval much shorter than tunneling time.

To be treated as an eigenstate, the $\psi_S(q,t)$ must have either long tunneling time τ or small tunnel splitting $\Delta\epsilon$. As the amplitude of the driving force is increased, the tunneling time of the wave packet $\psi_S(q,0)$ is also increased. On the one hand, good conditions for the degeneration of a doublet implies strong localization of $\psi(q,0)$ in one of the double wells. Therefore, Fig. 6 confirms it indirectly by revealing this clearly, or rather, the localization of the wave packet $\psi_S(q,0)$ is reinforced with the increase of the amplitude of the driving force as it was reinforced with the increase of the thickness of the central barrier. When $F=2.5$, the wave packet of $\psi_S(q,0)$ is most strongly localized around the stable fixed point of period-1/2 resonance generated in the left side well. This is verified because the generating condition of the period-1/2 resonance improves with the increase of the amplitude of the driving force.

Figure 7(a) shows that the condition of the degeneration of $\psi_S(q,0)$ is better satisfied when the central potential barrier is thick. In Fig. 7, the filled circles represent the values of the splitting of the doublet, $\Delta\epsilon=|\epsilon_{41}-\epsilon_{40}|$, associated with the stable fixed point of the period-1/2 resonance. In the classical limit, period-1/2 resonance describes the properties of a particle oscillating with a period 1/2 within only one of the double wells. Therefore, in the quantum system, the role of period-1/2 resonance is revealed when the blocking effect of tunneling through the central potential barrier becomes strong.

Figure 7(b) shows that the condition of the degeneration of $\psi_S(q,0)$ is also better satisfied when the amplitude of the driving force is increased. Tunneling times between resonant islands usually increase smoothly with the increase of the amplitude of the driving force, although tunneling times at certain amplitudes of the driving force are erratic due to chaos-induced avoided level crossing. For example, when $F=4.2$ and 5.4. However, in this system, suppression of tunneling occurs when the degenerated Floquet states are localized and the dynamical quasidegeneracies arise due to nonlinear resonances. This result is different from that reported by Lin and Ballentine [12] because of our concern for a specific system whose central potential barrier is very thin. Besides, the degenerated Floquet states are less affected by avoided crossing because, in this paper, we treat the system in the region of the amplitude of the driving force F smaller than the critical value $F_c\simeq 12.5$ associated with global chaos by resonance overlap. That is, we treat a weakly chaotic system. Therefore, in our system, with the increase of the amplitude of the driving force, the global characteristics of the system are decided by the enhanced effect of the central potential barrier that was extremely weak in the absence of the driving force.

Now, although this mechanism of suppressed tunneling is similar to that observed by Grossmann *et al.* [14–17], the origins of the two mechanisms are somewhat different from each other. Suppressed tunneling under the conditions of Grossmann *et al.* is a very general behavior in the deep quantum regime that can occur even in a two level system [34]. The perturbation of the driving force on the classical motion of the system is observed to have a minor effect [34]. The case reported by Grossmann *et al.* is therefore an example of intrinsic quantum control of tunneling in the deep quantum regime. However, tunnel suppression in our model becomes dominant in the classical regime rather than in the deep quantum regime. That is, in our model, the mechanism of the suppressed tunneling is ascribed to the increased effect of the role of the central potential barrier as the amplitude of the driving force is increased.

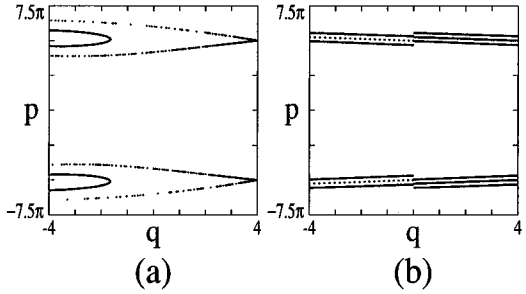

FIG. 8. Classical Poincaré surface of section in a driven single or double square-well system is drawn in (a) or (b), respectively. The regular islands are clear in (a) but not in (b). (a) $(T=1,\ F=2.5,\ 2b=0.00,\ \mu=1,\ \hbar=1,\ 2a=8,\ V_0=0)$, (b) $(T=1,\ F=2.5,\ 2b=0.03,\ \mu=1,\ \hbar=1,\ 2a=8,\ V_0=500)$.

B. Tunnel enhancement induced by a period-1 resonance

The result of enhanced tunneling, i.e., the oscillatory motion of $|\psi(q,t)|^2$ through the central barrier between the double wells at the time interval (3,6) is outlined in Fig. 1. It can be explained by the property of the stable fixed point of the period-1 resonance generated through the central potential barrier by the driving force, $F_0=-F\cos(2\pi t/1)$.

When the system is driven by $F_0(t)=-2.5\cos(2\pi t/1)$, the island of the period-1 resonance is clearly manifested in the Poincaré surface of section of Fig. 8(a) where the system has no central potential barrier, i.e., $2b=0.00$. Whereas, it is not manifested in the Poincaré surface of section of Fig. 8(b) where the system has a central potential barrier of thickness $2b=0.03$. To more clearly show the property of the period-1 resonance quantum mechanically, Husimi functions of some Floquet states of the period-1 resonance are drawn in Figs. 9(a) and 9(b), where they are calculated for the same value of the system parameters as those used in Figs. 8(a) and 8(b), respectively. Without the central potential barrier, as in Fig. 9(a), the Floquet states evidently manifest the trace of the period-1 resonance [35]. On the one hand, although the thickness of the central potential barrier is not zero as $2b=0.03$, the trace of the period-1 resonance is still retained in Fig. 9(b).

A single square-well system is an extreme case of a double square-well system whose central potential barrier has disappeared. In the single square-well system the generation of period-1 resonance is evident when the system is driven by a sinusoidal force of a period 1 [35]. The property of the nonlinear resonance is gradually destroyed as the role of the central potential barrier appears. For sufficiently thin

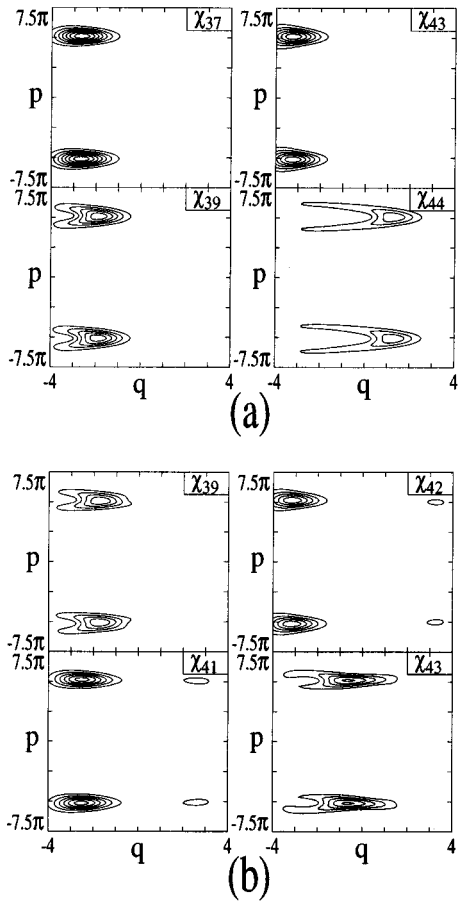

FIG. 9. The Husimi functions of some Floquet states compared with the classical Poincaré surface of sections of Fig. 8. The shape of tori of regular islands of nonlinear resonance shown on the Husimi functions as drawn in (b) is evident, but its trace is still retained on those in (a). The χ_{43} of (a) and χ_{42} of (b) are, respectively, the Floquet states associated with the property of the stable fixed points of the period-1 resonance of Fig. 8(a). The Husimi functions are calculated for the same values of the system parameters as in Figs. 8(a) and 8(b).

central potential barrier, the property of the Floquet state pertaining to the stable fixed point of period-1 resonance is slightly destructed and retained, because the property of the stable fixed point described by a local miminum of the pendunlum potential (or the potential related to the Mathieu equation) [35,36] which is induced by the driving force, is robust against any perturbation of the system parameters, i.e., the thickness of the central potential barrier, the amplitude of the driving force, and so on. As a consequence, in the presence of the central potential barrier, we can observe the properties of the period-1 resonance induced in the double square-well system in Fig. 9(b).

Another purpose of this paper is to make the property of time evolution of an initial wave packet $\psi(q,t)$ follow the dynamical property of the one Floquet state $\psi_E(q,t)$ associated with the stable fixed point of period-1 resonance. As an example, the state of $\psi_E(q,t=0)$ is given by the χ_{42} of Fig. 9(b) if $F=2.5$, $2b=0.03$. In this case, the property of the state of $\psi_E(q,t)$ associated with the stable fixed point also stands for the global property of an island of period-1 reso-

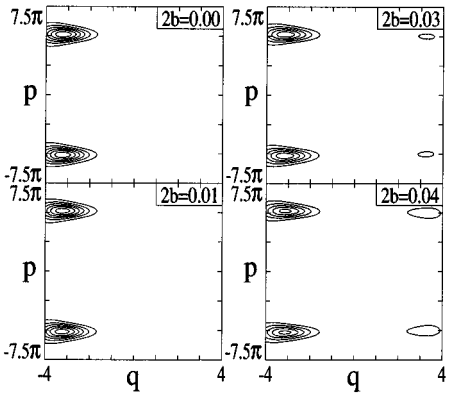

FIG. 10. Observation of the localization of the Husimi function of a wave packet of $\psi_E(q,0)$ associated with χ_{42} in Fig. 9(b). When the amplitude of thickness of the central potential barrier is increased as $2b=0.00$, 0.01, 0.03, and 0.04, the Husimi function is more weakly localized around the stable fixed point of the period-1 resonance. ($T=1$, $F=2.5$, $\mu=1,\hbar=1$, $2a=8$, $V_0=500$).

nance. Thus we are mainly concerned with the time evolution of the wave packet of $\psi_E(q,t)$ associated with the stable fixed point. Figure 10 shows that the Husimi functions of the one Floquet state, $\psi_E(q,t=0)$, associated with the stable fixed point of period-1 resonance, are less localized in the left well with the increase of the thickness of the central potential barrier as $2b=0.00$, 0.01, 0.03, 0.04. Consequently, the pattern of the regular island of period-1 resonance is presented most poorly by the Husimi function in case $2b=0.04$. This is explained by the fact that the generating condition of the period-1 resonance becomes worse with the increase of the role of tunnel blocking of the central potential barrier. This also implies that the wave packet of $\psi_E(q,t)$ still attributes to period-1 resonance making the wave packet oscillate through the central barrier within double-well potential only if the thickness of the central barrier is thin. So, we can observe the oscillatory motion of a wave packet that mimics the attribution of the stable fixed point of period-1 resonance in the single square-well system.

Since the wave packet of $\psi_E(q,t)$ is given by even parity in our system, it satisfies the following dynamical symmetry [10]:

$$\psi_E(q,nT)=\psi_E(q,t=0), \tag{10}$$

$$\psi_E(q,nT+T/2)=\psi_E(-q,t=0). \tag{11}$$

To clarify the properties of the dynamical symmetry of the wave pakcet of $\psi_E(q,t)$ in Fig. 11, we observe a variety of motions of one wave packet obtained in case $2b=0.03$, $T=1$ and $F=2.5$. Thus, for the full description of tunneling properties exhibited by a system with a dynamical symmetry, we observe the Husimi function of the wave packet of $\psi_E(q,t)$ when they correspond to integral multiples of the half period of the driving force in Fig. 11(a). It confirms the validity of Eqs. (10) and (11) which indicate that $\psi_E(q,nT)$ is exactly equal to $\psi_E(q,0)$ and $\psi_E(q,nT+T/2)$ is given by $\psi_E(-q,0)$. Figure 11(b) shows the detailed descriptions of the dynamical motion of the wave packet of

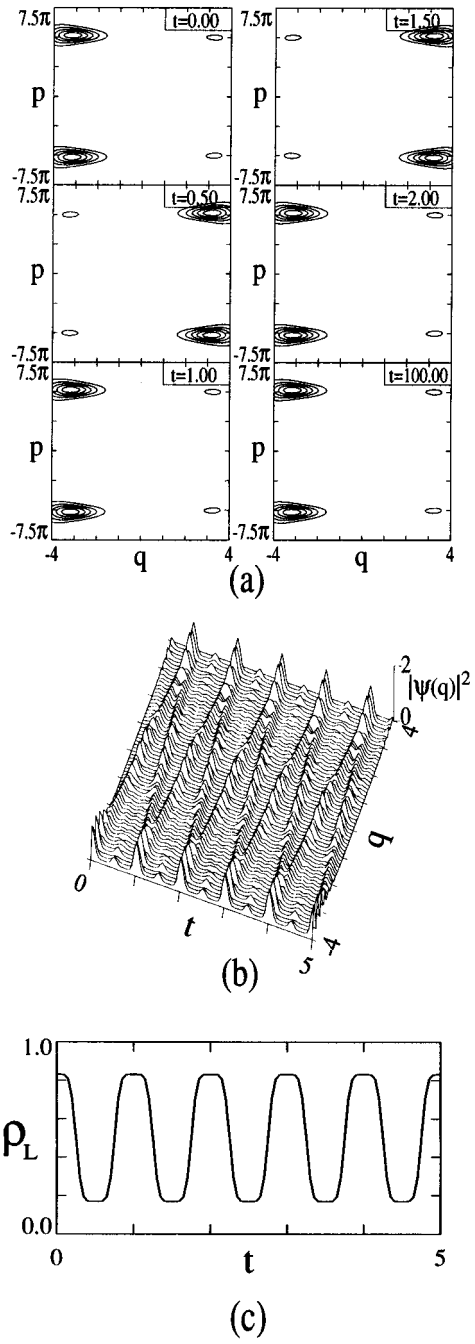

FIG. 11. Time evolution of a wave packet of $\psi_E(q,t)$ chosen in Fig. 10 in case $2b=0.03$. Husimi functions of $\psi_E(q,t)$ at selected times corresponding to integral multiples of the half period of the driving force are drawn in (a). The time evolution of $|\psi_E(q,t)|^2$ for short time intervals is drawn in (b). The occupation probability in the left well $\rho_L(t)$ is drawn in (c). The detailed descriptions are given in the contents. ($T=1$, $F=2.5$, $2b=0.03$, $\mu=1$, $\hbar=1$, $2a=8$, $V_0=500$).

$\psi_E(q,t)$. The motion of the wave packet can be described by the fast oscillation having the same period 1 as the driving force. The fast oscillation of a period $T=1$ can be understood as having a relation to the classical oscillation of a particle in the absence of the central barrier. To present the property of tunneling more clearly, we plot the occupation probability $\rho_L(t)$ in Fig. 11(c). The oscillatory motion of $\rho_L(t)$ with a period 1 continues without undergoing any dissipation.

On the one hand, the wave packet of $\psi_E(q,t=0)$ becomes more strongly localized about the stable fixed point of period-1 resonance generated by increasing the amplitude of the driving force though it was not shown in this paper. This is revealed when the generating condition of the period-1 resonance is improved by the increase of the amplitude of the driving force.

The tunneling rate of the wave packet of $\psi_E(q,t)$ undergoing enhanced tunneling by the period-1 resonance is inversely proportional to the amplitude of the thickness of the central potential and proportional to the amplitude of the driving force. In other words, the amplitude of the oscillation of $\rho_L(t)$ is reduced with the increase of the amplitude of the thickness of the central potential barrier $2b$. The amplitude is raised with the increase of the amplitude of the driving force F. Since this tunneling is induced by the role of nonlinear resonances, the tunneling rate is enhanced by the increase of the amplitude of the driving force.

In summary, the tunneling rate of $\psi_E(q,t)$ is increased by reinforcing the role of period-1 resonance. However, it is different from the dc resonantly enhanced tunneling in quantum wells which exhibits a drastic reduction of the tunneling time in an asymmetric double-well system when the ground state of the one well is aligned with an excited state of the other well by applying a dc electric field [37–40].

C. Application on tunnel controlling

So far, we have discussed the mechanism of suppressed tunneling and enhanced tunneling. For the tunneling of a wave packet of $\psi(q,t)$ to be effectively suppressed by the period-1/2 resonance, this wave packet must resemble the wave packet of $\psi_S(q,t)$. On the one hand, for the tunneling of a wave packet of $\psi(q,t)$ to be effectively enhanced by the period-1 resonance, this wave packet needs to resemble the wave packet of $\psi_E(q,t)$. Henceforth, for optimum control of the wave packet of $\psi(q,t)$, it is required that the $\psi_S(q,t)$ and the $\psi_E(q,t)$ have similar forms.

To find a tendency on the change of the difference between $\psi_S(q,t=0)$ and $\psi_E(q,t=0)$ when the amplitude of the driving force is increased, we present the shapes of the $\psi_S(q,t=0)$ and the $\psi_E(q,t=0)$ for $F=2.5$ and $F=5.8$ in Figs. 12(a) and 12(b), respectively, where c_n's are the coefficients that represent the amplitude of the projection of a wave packet of $\psi_S(q,0)$ and $\psi_E(q,0)$ on the eigenfuction $u_n(q)$ of H_0, i.e., $\psi_S(q,0)=\Sigma c_n u_n(q)$ or $\psi_E(q,0)=\Sigma c_n u_n(q)$. The $\psi_S(q,0)$'s and the $\psi_E(q,0)$'s are presented in the left and right side of Fig. 12. For the $F=2.5$ of Fig. 12(a), the difference between two wave packets is large. To illustrate, the amplitudes of c_{40}, c_{42} of $\psi_S(q,0)$ and the amplitudes of c_{39}, c_{41} of $\psi_E(q,0)$ are large. Whereas, the amplitudes of c_{39}, c_{41} of $\psi_S(q,0)$ and the amplitudes of c_{41}, c_{42} of $\psi_E(q,0)$ are not large. Therefore, the amplitude $\langle\psi_S(q,0)|\psi_E(q,0)\rangle=0.62$ is considerably smaller than 1. But, for the $F=5.8$ of Fig. 12(b), the difference between two wave packets is greatly reduced. For example, the amplitudes of c_{39}, c_{41}, c_{43} of the $\psi_S(q,t)$ and the $\psi_E(q,0)$ are simultaneously large. This shows the amplitude

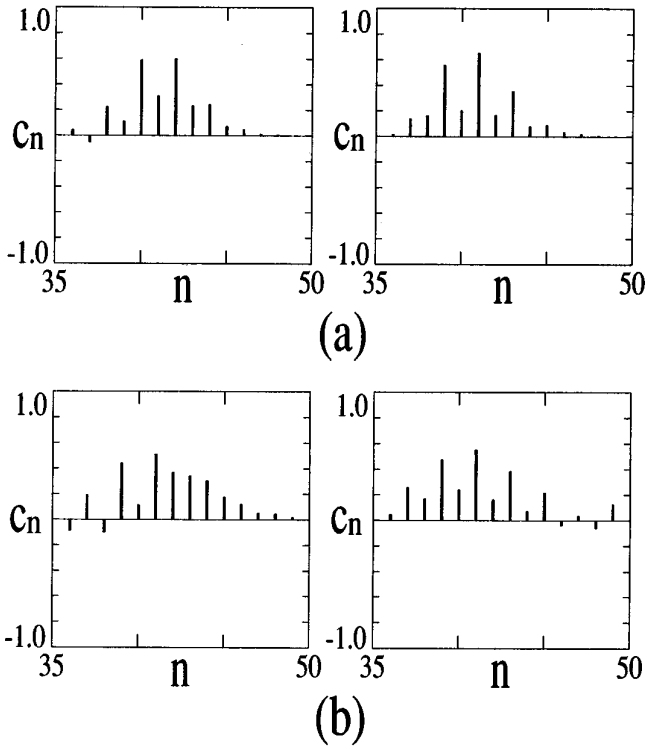

FIG. 12. The shapes of $\psi_S(q,t=0)$ and $\psi_E(q,t=0)$ when $F=2.5$ and $F=5.8$ are presented in (a) and (b), respectively, where c_n's are the coefficients of the amplitude of the projection of a wave packet of ψ_S and ψ_E on the eigenfunction u_n of H_0, i.e. $\psi_S=\Sigma c_n u_n(q)$ or $\psi_E=\Sigma c_n u_n(q)$. $\psi_S(q,0)$'s and $\psi_E(q,0)$'s are presented in the left and right side of the figure, respectively.

$\langle \psi_S(q,0)|\psi_E(q,0)\rangle = 0.81$ to also be large. Consequently, the resemblance between two wave packets is even greater in the large amplitude of the drving force $F=5.8$. In addition, the tunneling time τ of $\psi_S(q,0)$ is longer in the case where $F=5.8$. In other words, the tunnel splitting $\Delta\epsilon$ is smaller as Fig. 7(b) illustrates. So, if we want to control the tunneling of a wave packet of $\psi(q,t)$ as in Fig. 1, we must choose the wave packet of $\psi(q,t=0)$ by the linear combination of $\psi_S(q,0)$ and $\psi_E(q,0)$, i.e., $\psi(q,t=0)=[\psi_S(q,0)+\psi_E(q,0)]/\sqrt{2}$. Then, as observed in Fig. 1, tunnel controlling is more effective in the case where $F=5.8$ rather than when $F=2.5$.

Now, the amplitude of tunnel splitting associated with $\psi_S(q,t)$ may be large due to chaos-induced avoided level crossing [13] around a certain amplitude of the driving force of $F=4.2$ or 5.6 as shown in Fig. 7(b). Then, the localization of the doublet state may be broken. The localization of the eigenstate of enhanced tunneling, $\psi_E(q,t)$, may also be broken at a certain amplitude of the driving force due to chaos-induced avoided level crossing. With the increase of the amplitude of the driving force, the occurring frequency of this avoided level crossing increases as the chaotic region in the Poincaré surface of section grows. As a result, we cannot simply choose the large amplitude of the driving force to control the tunneling of the wave packet. We have to properly choose the system parameters that are unrelated to the avoided level crossing.

V. CONCLUSIONS

In this paper, we studied that the generation of nonlinear resonance is responsible for the change of tunneling in a driven double square-well system when its central potential barrier is very tall and very thin. When a classical nonlinear system is perturbed by a sinusoidal driving force, the system manifests many patterns of resonance islands and consequently it becomes more stable. This same mechanism was observed in our model system associated with quantum tunneling. That is, without the driving force, the generating condition of the period-1/2 resonance is poor due to the tunneling effect through the central potential barrier, and the generating condition of the period-1 resonance is also poor as a result of the blocking effect of tunneling through the central potential barrier. But, if our system is perturbed by the driving force, the traces of nonlinear resonances are manifested, and consequently the tunneling rate through the central potential barrier is changed. We observed that the direction of change of the tunneling rate is the same as that of the good condition for nonlinear resonance. Therefore, the generation of nonlinear resonance also plays an important role in a quantum tunneling system without classical counterpart. In particular, we studied the properties of the Floquet states associated with the stable fixed point that stands for the regular island of a nonlinear resonance and showed the possibility of tunnel controlling by changing the properties.

ACKNOWLEDGMENTS

I gratefully acknowledge discussions with Professor H. W. Lee. This research is supported by the KAIST Research Grant.

[1] S. Tomsovic and D. Ullmo, Phys. Rev. E **50**, 145 (1994).
[2] R. Roncaglia, L. Bonci, F. M. Izrailev, B. J. West, and P. Grigolini, Phys. Rev. Lett. **73**, 802 (1994).
[3] J. Plata and J. M. Gomez Llorente, J. Phys. A **25**, L303 (1992).
[4] A. Shudo and K. S. Ikeda, Phys. Rev. Lett. **74**, 682 (1995).
[5] T. M. Fromhold, P. B. Wilkinson, F. W. Sheard, L. Eaves, J. Miao, and G. Edwards, Phys. Rev. Lett. **75**, 1142 (1995).
[6] R. Utermann, T. Dittrich, and P. Hänggi, Phys. Rev. E **49**, 273 (1994).
[7] S. Chaudhuri and D. S. Ray, Phys. Rev. E **47**, 80 (1993).
[8] M. J. Davis and E. J. Heller, J. Chem. Phys. **75**(1), 246 (1981).
[9] W. A. Lin and L. E. Ballentine, Phys. Rev. Lett. **65**, 2927 (1990).
[10] A. Peres, Phys. Rev. Lett. **67**, 158 (1991).

[11] W. A. Lin and L. E. Ballentine, Phys. Rev. Lett. **67**, 159 (1991).
[12] W. A. Lin and L. E. Ballentine, Phys. Rev. A **45**, 3637 (1992).
[13] M. Latka, P. Grigolini, and B. J. West, Phys. Rev. A **50**, 1071 (1994).
[14] F. Grossmann, T. Dittrich, P. Jung, and P. Hänggi, Phys. Rev. Lett. **67**, 516 (1991).
[15] F. Grossmann, T. Dittrich, and P. Hänggi, Physica B **175**, 293 (1991).
[16] F. Grossmann, P. Jung, T. Dittrich, and P. Hänggi, Z. Phys. B **84**, 315 (1991).
[17] T. Dittrich, F. Grossmann, P. Jung, B. Oelschlägel, and P. Hänggi, Physica A **194**, 173 (1993).
[18] R. Bavli and H. Metiu, Phys. Rev. Lett. **69**, 1986 (1992).
[19] D. Farrelly and J. A. Milligan, Phys. Rev. E **47**, R2225 (1993).
[20] H. W. Lee, Phys. Rep. **259**, 147 (1995).
[21] K. Husimi, Proc. Phys. Math. Soc. Jpn. **22**, 264 (1940).
[22] K. Takahashi and N. Saito, Phys. Rev. Lett. **55**, 645 (1985).
[23] Ya. B. Zel'dovich, Zh. Éksp. Teor. Fiz. **51**, 1492 (1966) [Sov. Phys. JETP **24**, 1006 (1967)].
[24] H. Sambe, Phys. Rev. A **7**, 2203 (1973).
[25] Ya. B. Zel'dovich, Usp. Fiz. Nauk. **110**, 139 (1974) [Sov. Phys. Usp. **16**, 427 (1974)].
[26] J. Y. Shin and H. W. Lee, Phys. Rev. E **53**, 3096 (1996).
[27] G. M. Zaslavsky, Phys. Rep. **80**, 157 (1981).
[28] D. F. Escande, Phys. Rep. **121**, 165 (1985).
[29] F. Haake, M. Kuś, and R. Scharf, Z. Phys. B **65**, 381 (1987).
[30] B. C. Sanders and G. J. Milburn, Z. Phys. B **77**, 497 (1989).
[31] O. Bohigas, S. Tomsovic, and D. Ullmo, Phys. Rev. Lett. **64**, 1479 (1990); **65**, 5 (1990).
[32] O. Bohigas, S. Tomsovic, and D. Ullmo, Phys. Rep. **223**, 43 (1993).
[33] M. Latka, P. Grigolini, and B. J. West, Phys. Rev. A **47**, 4649 (1993).
[34] J. M. Gomez Llorente and J. Plata, Phys. Rev. A **45**, R6958 (1992).
[35] J. Y. Shin and H. W. Lee, Phys. Rev. E **50**, 902 (1994).
[36] W. A. Lin and L. E. Reichl, Phys. Rev. A **37**, 3972 (1988).
[37] K. Leo, J. Shah, E. O. Göbel, T. C. Damen, S. Schmitt-Rink, W. Schäfer, and K. Köhler, Phys. Rev. Lett. **66**, 201 (1991).
[38] R. Rouse, S. Han, and J. E. Lukens, Phys. Rev. Lett. **75**, 1614 (1995).
[39] D. Y. Oberli, J. Shah, T. C. Damen, C. W. Tu, T. Y. Chang, D. A. B. Miller, J. E. Henry, R. F. Kopf, N. Sauer, and A. E. DiGiovanni, Phys. Rev. B **40**, 3028 (1989).
[40] G. Livescu, A. M. Fox, D. A. B. Miller, T. Sizer, and W. H. Knox, Phys. Rev. Lett. **63**, 438 (1989).